Charge-Kondo effect mediated by repulsive interactions

S. Mojtaba Tabatabaei
Department of Physics, Shahid Beheshti University, Evin, Tehran 19839, Iran

(Received 1 April 2018; revised manuscript received 3 June 2018; published 18 June 2018)

We investigate the Kondo effect in a double quantum dot which is capacitively coupled to a charge qubit. It is shown that due to this capacitive coupling, the bare interdot repulsive interaction in the double quantum dot is effectively reduced and eventually changed to an attractive interaction for strong couplings between the double quantum dot and the qubit. By deriving the low-energy effective Hamiltonian of the system, we find that the low-energy dynamics of the system corresponding to these two positive or negative effective interaction regimes can be described, respectively, by an isotropic orbital-Kondo or an anisotropic charge-Kondo Hamiltonian. Moreover, we study various thermodynamic and electronic transport properties of the system by using the numerical renormalization group method.

DOI: 10.1103/PhysRevB.97.235131

I. INTRODUCTION

During the last two decades, the Kondo effect in quantum dots (QDs) has become an attractive research field in condensed matter physics [1–10]. The main motivation for these studies is the possibility to explore various aspects of such an important effect in an experimentally accessible and fully tunable manner. Theoretically, the Kondo effect is expected to arise at low temperatures whenever a localized system with a degenerate ground state is coupled to an environment with the same degeneracy, and it is usually related to the formation of a zero-energy resonance state in the density of states of the system as a result of higher order tunneling processes between the localized system and the environment [1]. Depending on the nature of the degrees of freedom contributing to the manifestation of this effect, different kinds of Kondo effects have been identified in the literature. For example, the *spin*-Kondo effect is the most addressed Kondo effect, which is associated with the fluctuations in the degenerate spin-up and -down states in the local system [11–13]. Another example is the *orbital*-Kondo effect, which is formed in a double quantum dot (DQD) and associated with the degenerate pseudospin states corresponding to the occupation of the DQD by an electron in its left or right dot [14–16].

The other somehow elusive Kondo effect is the *charge*-Kondo effect, which is associated with the fluctuations in degenerate states with different charge occupations. In this sense, the charge-Kondo effect is expected to occur in negative-U centers where an attractive interaction makes the doubly occupied or empty states have lower energies than the singly occupied states. Despite the fact that the theory of charge-Kondo effect was developed in early 1990s [17], its experimental realization was not reached until recent years. It was first reported in bulk PbTe semiconductors doped with Tl valence-skipping atoms which are in essence acting as negative-U centers in the host material [18–21]. Another observation of the charge-Kondo effect was also reported in transport through single-electron transistors formed at $LaAlO_3/SrTiO_3$ interfaces [22–24]. Meanwhile, some efforts have been also devoted to engineer the attractive interaction required for the charge-Kondo effect by introducing other degrees of freedom interacting with electrons. References [25–33] are examples of such theoretical proposals.

Recently, Hamo *et al.* [34] reported the observation of attracting electrons in a setup composed of a carbon nanotube double quantum dot (DQD) along with a charge qubit, both of which are constructed on separate microchips, placed one above the other and perpendicular to each other. They found that an attractive interaction will be induced between the electrons in the DQD when the height of the qubit above the DQD becomes less than a specific value. The attraction mechanism in their setup, as is discussed by Little [35], is purely electronic and of excitonic origin: An electron on the DQD repels the electron in the up state of the qubit, leaving behind it a cloud of positive charge on the qubit; in turn, this positive charge will attract the other electron on the DQD, making the whole to be two attracting electrons on the DQD.

In view of the presence of attractive electrons in the DQD-qubit system, it is natural to ask whether or not the electronic transport through the DQD could show the charge-Kondo effect. It should be emphasized that in their experiment Hamo *et al.* observed a conductance enhancement on the degeneracy points between the two empty and doubly occupied states of the DQD, a signature which was assigned to the charge-Kondo effect by them. However, so far, there has not been presented a rigorous description for the Kondo effect in the DQD-qubit coupled system in the literature.

In the present work, we theoretically explore the characteristics of the Kondo effect in the DQD-qubit coupled system. In the rest of the paper, in Sec. II, we first introduce the model Hamiltonian of the DQD-qubit system and discuss the effective interaction induced in the DQD due to its coupling with the qubit. Then, in Sec. III, we derive the low-energy effective Hamiltonian of the system by using the Raleigh-Schrödinger degenerate perturbation theory [30,36]. We show that for positive effective interaction in the DQD the system exhibits isotropic orbital-Kondo effect, while in the negative effective interaction regime the anisotropic charge-Kondo effect will be manifested in the system at low enough temperatures. Then

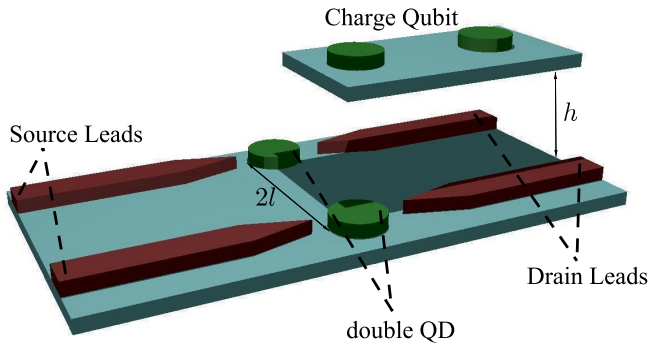

FIG. 1. The charge qubit is suspended above the DQD at height h and midway between the two dots of the DQD. Each dot of the DQD is coupled to its own source and drain electrodes and the distance between them is $2l$. One of the qubit's dots has smaller distance to the DQD than the second qubit's dot, and therefore the capacitive effect of the second dot of the qubit on the dynamics of the DQD is overestimated.

in Sec. IV we supplement our study with the results obtained by using the numerical renormalization group (NRG) method [37] to confirm the presence of these different Kondo effects in the system and extract some of the DQD's transport properties in the charge-Kondo regime. Finally, in Sec. V, we give the conclusions.

II. THE MODEL

Our model system, which is shown in Fig. 1, consists of a parallel DQD and a charge qubit. The qubit is placed on a separate host than the DQD and is positioned above the midpoint between DQD at height h, so that the DQD and the qubit can interact with each other only in a repulsive manner. The DQD is constituted from two dots, and each of them is contacted to its own source and drain electrodes. The total Hamiltonian of the system is given by

$$\hat{\mathcal{H}} = \hat{\mathcal{H}}_S + \hat{\mathcal{H}}_L + \hat{\mathcal{H}}_T. \tag{1}$$

The first term is the Hamiltonian of the DQD-qubit system, which is given by $\hat{\mathcal{H}}_S = \hat{\mathcal{H}}_{\rm DQD} + \hat{\mathcal{H}}_{\rm qubit} + \hat{\mathcal{H}}_I$. The Hamiltonian of the DQD is given by

$$\hat{\mathcal{H}}_{\rm DQD} = \varepsilon_1\hat{n}_1 + \varepsilon_2\hat{n}_2 + U\hat{n}_1\hat{n}_2, \tag{2}$$

where $\hat{n}_i = \hat{d}_i^\dagger\hat{d}_i$, $\hat{d}_i^\dagger$ for $i = 1,2$ creates an electron in the respective QD, ε_i is the applied gate voltage, and U is the interdot electron-electron interaction energy which is assumed to be a positive constant. In order to capture the main physics of the charge-Kondo effect, we consider the electrons to be spinless (by applying a large magnetic field) and therefore each QD can be occupied only by a single electron. Moreover, $\hat{\mathcal{H}}_{\rm qubit}$ denotes the Hamiltonian of the qubit, which is given by

$$\hat{\mathcal{H}}_{\rm qubit} = -\frac{\omega_0}{2}\hat{\tau}_z + \frac{\Delta}{2}\hat{\tau}_x, \tag{3}$$

where ω_0 is the energy difference between the energy levels on either dots of the qubit, $\Delta/2$ gives the corresponding electron hybridization in the qubit, and $\hat{\tau}_x$ and $\hat{\tau}_z$ are the usual Pauli operators operating in the qubit's Hilbert space and defined respectively by $\hat{\tau}_x = (|\Uparrow\rangle\langle\Downarrow| + |\Downarrow\rangle\langle\Uparrow|)$ and $\hat{\tau}_z = (|\Uparrow\rangle\langle\Uparrow| - |\Downarrow\rangle\langle\Downarrow|)$, where $|\Uparrow\rangle$ and $|\Downarrow\rangle$ represent the two charge states of the qubit. Furthermore, the interaction Hamiltonian of the DQD-qubit is given by

$$\hat{\mathcal{H}}_I = \frac{\lambda}{2}\hat{n}_d\hat{\tau}_z, \tag{4}$$

where $\hat{n}_d = \hat{n}_1 + \hat{n}_2$ and λ is the capacitive coupling energy between DQD and qubit, which is assumed to be a positive constant. The value of λ is proportional to r_λ^{-1}, where $r_\lambda = \sqrt{l^2 + h^2}$ is the distance between the charge qubit and the DQD (see Fig. 1 for the definitions of l and h).

The DQD is tunnel coupled to four normal metal electrodes so that each dot is coupled to its own source and drain electrodes. The electrodes are described by $\hat{\mathcal{H}}_L = \sum_{i,j}\hat{\mathcal{H}}_{L,i,j}$, where $j = S,D$ denote source and drain electrodes for the respective dots $i = 1,2$, and $\hat{\mathcal{H}}_{L,i,j} = \sum_k \varepsilon_k\,\hat{c}^\dagger_{k,i,j}\hat{c}_{k,i,j}$, where $\hat{c}^\dagger_{k,i,j}$ is the corresponding operator for electron creation with energy ε_k in the respective electrodes. The hybridization of each dot of the DQD with their electrodes is assumed to be energy independent and characterized by a hybridization constant t, and is described by $\hat{\mathcal{H}}_T = \sum_{k,i,j} t(\hat{c}^\dagger_{k,i,,j}\hat{d}_i + \text{H.c.})$. The Hamiltonian of each source and drain electrode corresponding to each dot may be transformed to the Hamiltonian of a single lead by using the canonical transformations $\hat{\tilde{c}}_{k,i} = (\hat{c}_{k,i,S} + \hat{c}_{k,i,D})/\sqrt{2}$ and $\hat{\tilde{b}}_{k,i} = (\hat{c}_{k,i,S} - \hat{c}_{k,i,D})/\sqrt{2}$, and then the expressions of the leads and the DQD-leads Hamiltonians are given, respectively, by

$$\hat{\mathcal{H}}_L = \sum_{k,i}\varepsilon_k\,\hat{\tilde{c}}^\dagger_{k,i}\hat{\tilde{c}}_{k,i} \tag{5}$$

and

$$\hat{\mathcal{H}}_T = \sum_{k,i} t(\hat{\tilde{c}}^\dagger_{k,i}\hat{d}_i + \text{H.c.}). \tag{6}$$

In order to learn more about the impact of the capacitive interaction between the DQD and qubit on the behavior of the system, it is useful to calculate the eigenstates and their energies of the isolated DQD-qubit system. The eigenenergies of $\mathcal{H}_S$ are obtained straightforwardly from $\mathcal{H}_S|\psi_\pm^{n_1,n_2}\rangle = E_\pm^{n_1,n_2}|\psi_\pm^{n_1,n_2}\rangle$, as

$$E_\pm^{n_1,n_2} = n_1\varepsilon_1 + n_2\varepsilon_2 + n_1n_2U \pm \frac{\Omega_{n_d}}{2}, \tag{7}$$

where $n_d = n_1 + n_2$ is the total occupation of the DQD and $\Omega_n = \sqrt{\Delta^2 + (\omega_0 - n\lambda)^2}$. Moreover, the eigenstates are found to be $|\psi_\pm^{n_1,n_2}\rangle = |n_1,n_2\rangle_{\rm DQD}|n_d,\pm\rangle_{\rm qubit}$, where $|n_1,n_2\rangle_{\rm DQD}$ is the occupation state of DQD and $|n_d,\pm\rangle_{\rm qubit}$ is the qubit eigenstate given by

$$|n_d,\pm\rangle_{\rm qubit} = b_\pm^{n_d}[(-\omega_0 + n_d\lambda \pm \Omega_{n_d})|\Uparrow\rangle + \Delta|\Downarrow\rangle], \tag{8}$$

where $b_\pm^{n_d}$ is a normalization constant. Looking at the eigenenergies, Eq. (7), we can understand that as a direct consequence of the coupling with qubit, the electron-electron interaction in DQD is reduced to an effective interaction equal to

$$\begin{aligned} U_{\rm eff} &= E_-^{1,1} + E_-^{0,0} - E_-^{1,0} - E_-^{0,1} \\ &= U + \Omega_1 - \tfrac{1}{2}(\Omega_2 + \Omega_0). \end{aligned} \tag{9}$$

More interestingly, we see that when $U < \frac{1}{2}(\Omega_2 + \Omega_0) - \Omega_1$, the sign of $U_{\rm eff}$ becomes negative, which means that in such situations there is a net attractive interaction between the electrons in the DQD. Even though it may seem surprising at first glance, we can get some sense of this attractive interaction by noting that this is indeed an induced attraction between the electrons. In other words, the presence of the oscillating polarization field of the qubit on the electrons in the DQD dresses their electric potential and forces them to favor the doubly occupied states more than the singly ones, which in turn can be considered as the two electrons attracting each other [34,35].

Another feature in Eq. (7) is that, for some particular parameter configurations, the ground state of the system becomes degenerate, composed of the two states $|\psi_-^{0,1}\rangle$ and $|\psi_-^{1,0}\rangle$ ($|\psi_-^{0,0}\rangle$ and $|\psi_-^{1,1}\rangle$) in the $U_{\rm eff} > 0$ ($U_{\rm eff} < 0$) regime. Accordingly, we can expect that when the subsystem of the DQD qubit with the degenerate ground state is appropriately coupled to the electrodes, higher order electron tunneling processes between DQD and electrodes dress this degenerate state and form a many-body Kondo resonance, and hence a Kondo effect arises in the system.

III. LOW-ENERGY EFFECTIVE HAMILTONIAN

In order to identify the characteristics of the Kondo effect in our model system, it is sufficient to derive a low-energy effective Hamiltonian describing the low-temperature dynamics of the system up to the second order of the electron tunneling processes in the DQD. Here, we present the main results and relegate the technical details to the Appendix. By using the projection operators

$$\hat{P}_\pm^{n_1,n_2} = |\psi_\pm^{n_1,n_2}\rangle\langle\psi_\pm^{n_1,n_2}|, \tag{10}$$

we can calculate the effective Hamiltonian of the system by using [30,36]

$$\hat{\mathcal{H}}_{\rm eff} = \sum_{\substack{n_1,n_2=0,1\\ \nu=\pm}} \frac{\hat{P}_0\hat{\mathcal{H}}_T\hat{P}_\nu^{n_1,n_2}\hat{\mathcal{H}}_T\hat{P}_0}{E_0 - E_\nu^{n_1,n_2}}, \tag{11}$$

where $\hat{P}_0$ and E_0 are the corresponding projector operator and energy of the ground state of the unperturbed system, respectively.

In the positive $U_{\rm eff}$ regime, the ground state of the system can become degenerate (which is essential for the Kondo effect to be arisen in the system) and constituted from the two states $|\psi_-^{0,1}\rangle$ and $|\psi_-^{1,0}\rangle$ when the conditions $\lambda = \omega_0$, $\varepsilon_1 + U/2 = \varepsilon_2 + U/2 = V_g$, and $|V_g| < U_{\rm eff}/2$, are satisfied. Then, using Eq. (11), the low-energy effective Hamiltonian can be obtained by

$$\begin{aligned}\hat{\mathcal{H}}_{\rm eff} &= \sum_{\substack{n_1,n_2=0,1\\ \nu=\pm}} \frac{(\hat{P}_-^{1,0} + \hat{P}_-^{0,1})\hat{\mathcal{H}}_T\hat{P}_\nu^{n_1,n_2}\hat{\mathcal{H}}_T(\hat{P}_-^{1,0} + \hat{P}_-^{0,1})}{E_-^{1,0} - E_\nu^{n_1,n_2}} \\ &\approx J\,\vec{S}_d\cdot\vec{S}_c,\end{aligned} \tag{12}$$

where $\vec{S}_d$ and $\vec{S}_c$ are the corresponding pseudospin vector of DQD and electrodes, respectively, which are defined in Eq. (A7), and J is the Kondo exchange coupling constant which is given by

$$J = \frac{t^2}{(V_g+U) - \frac{(\lambda/2)^2}{\Delta+V_g+U}} - \frac{t^2}{V_g - \frac{(\lambda/2)^2}{V_g-\Delta}}, \tag{13}$$

which is always positive valued within the above mentioned parameter regime. Thus, we see that the low-temperature dynamics of the system in the $U_{\rm eff} > 0$ regime is governed by a $SU(2)$ isotropic orbital-Kondo Hamiltonian in which a single electron on the DQD plays the role of a pseudospin making a singlet state with the corresponding pseudospins of the electrodes. The Kondo temperature, which is the particular temperature below which the Kondo effect is manifested in the system, is given in this case by

$$T_K^i = \alpha \exp\left[-\frac{1}{\rho_0 J}\right], \tag{14}$$

where α is a proportionality constant and $\rho_0 = 1/(2D)$ is the density of states of the leads, which is assumed to be constant in the wide-band approximation, and D is the half-bandwidth of the electrodes. To the lowest order in λ, the correction to the value of J equals

$$\begin{aligned}J \approx &-\frac{t^2U}{V_g(V_g+U)} + \frac{t^2(\lambda/2)^2}{(V_g+U)^2(\Delta+V_g+U)} \\ &+ \frac{t^2(\lambda/2)^2}{V_g^2(\Delta-V_g)} + \mathcal{O}(\lambda^4).\end{aligned} \tag{15}$$

Hence, in the positive $U_{\rm eff}$ regime, the DQD-qubit coupling results in an enhancement of the Kondo temperature of the system. Note that for $\lambda = 0$, Eq. (13) correctly reproduces the results of the conventional orbital-Kondo effect in a DQD.

For the negative $U_{\rm eff}$ regime, by demanding the ground state to be degenerate and constituted from the two states $|\psi_-^{0,0}\rangle$ and $|\psi_-^{1,1}\rangle$, it can be found that the the sufficient conditions are $\lambda = \omega_0$, $\varepsilon_1 + \varepsilon_2 + U = 0$ and $|V_z| < -U_{\rm eff}/2$, where $V_z = \varepsilon_1 + U/2 = -(\varepsilon_2 + U/2)$. Now, we can perform a second-order perturbation to obtain the low-energy effective Hamiltonian of the system as

$$\begin{aligned}\hat{\mathcal{H}}_{\rm eff} &= \sum_{\substack{n_1,n_2=0,1\\ \nu=\pm}} \frac{(\hat{P}_-^{0,0} + \hat{P}_-^{1,1})\hat{\mathcal{H}}_T\hat{P}_\nu^{n_1,n_2}\hat{\mathcal{H}}_T(\hat{P}_-^{0,0} + \hat{P}_-^{1,1})}{E_-^{0,0} - E_\nu^{n_1,n_2}} \\ &\approx \left[J_\parallel I_d^z I_c^z + J_\perp\left(I_d^x I_c^x + I_d^y I_c^y\right)\right],\end{aligned} \tag{16}$$

where $\vec{I}_d$ ($\vec{I}_c$) are the corresponding isospin operators of the DQD (electrodes) which are defined by applying a special particle-hole transformation, i.e., $d_2^\dagger \to d_2$ and $\tilde{c}_{k,2}^\dagger \to -\tilde{c}_{k,2}$, on the $\vec{S}_d$($\vec{S}_c$) operators and are given in Eq. (A10). Furthermore, the two parallel and transverse exchange Kondo coupling constants $J_\parallel$ and $J_\perp$ are given by

$$\begin{aligned}J_\parallel = 2t^2\Bigg[&\frac{-\lambda + U + 2V_z - \frac{\Delta^2(\lambda+2\Omega_0)}{\Delta^2+\lambda^2+\lambda\Omega_0}}{(U+2V_z-\Omega_0)^2 - \Delta^2} \\ &- \frac{\lambda - U + 2V_z + \frac{\Delta^2(\lambda+2\Omega_0)}{\Delta^2+\lambda^2+\lambda\Omega_0}}{(-U+2V_z+\Omega_0)^2 - \Delta^2}\Bigg],\end{aligned} \tag{17a}$$

$$J_\perp = \frac{2\Delta t^2}{\Omega_0}\left(\frac{1}{2V_z - U + \frac{\lambda^2}{2V_z - U + 2\Omega_0}} - \frac{1}{2V_z + U + \frac{\lambda^2}{2V_z + U - 2\Omega_0}}\right). \quad (17b)$$

Thus, the low-energy dynamics of the DQD-qubit system in the $U_{\rm eff} < 0$ regime is governed by an anisotropic charge-Kondo Hamiltonian. In this case, the Kondo temperature is given by [32]

$$T_K^a = \beta\left(\frac{J_\parallel + \sqrt{J_\parallel^2 - J_\perp^2}}{J_\parallel - \sqrt{J_\parallel^2 - J_\perp^2}}\right)^{-\frac{1}{4\rho_0\sqrt{J_\parallel^2 - J_\perp^2}}}, \quad (18)$$

where β is a proportionality constant.

We note that within the above particular range of parameter values, the system is always in the Kondo regime and relaxing these conditions can lead to a quantum phase transition into other fixed points of the system.

IV. NUMERICAL RENORMALIZATION GROUP RESULTS

Here, we provide numerical results obtained by the numerical renormalization group (NRG) method to confirm the manifestation of the Kondo effect in the DQD-qubit system. The NRG results are obtained using the NRG LJUBLJANA package [38] by solving the total Hamiltonian in Eq. (1) with $\Gamma = \pi\rho_0 t^2 = 0.01D$, where $\rho_0 = 1/(2D)$ is the density of states of the leads which is assumed to be constant in the wide-band approximation and $D = 1$ is taken as the unit of the energy scales. Moreover, we take $U = 20\Gamma$ and $\Delta = 10\Gamma$. We mention that for the chosen values of U and Δ, the particular value of λ at which $U_{\rm eff}$ will vanish is $\lambda \approx 28\Gamma$. Thus, the system is expected to be in the positive (negative) $U_{\rm eff}$ regime when $\lambda < 28\Gamma(\lambda > 28\Gamma)$.

First, we investigate the thermodynamic properties of the system. In Fig. 2, we show the temperature dependence of the impurity contribution on the entropy $S_{\rm imp}(T)$, on the orbital pseudospin magnetic susceptibility $\chi^S_{\rm imp}(T) = [\langle(S^z)^2\rangle - \langle(S^z)^2\rangle_0]/T$, where $S^z = S^z_d + S^z_c$ and $\langle\cdots\rangle_0$ denotes the thermal expectation value in the absence of the DQD and qubit, and on the total charge susceptibility $\chi^C_{\rm imp}(T) = [\langle Q^2\rangle - \langle Q^2\rangle_0]/T$ of the system in the p-h symmetric point and for several λ values corresponding to the both $U_{\rm eff} > 0$ and $U_{\rm eff} < 0$ regimes. As seen in Figs. 2(a) and 2(b), at high temperatures the system is in its free orbital fixed point where all 2^3 states of the DQD-qubit system are equally probable and hence the entropy becomes $S_{\rm imp} = k_B \ln 8$. By decreasing the temperature, the system crosses over to a local moment fixed point with $S_{\rm imp} = k_B \ln 2$, which means the presence of only two degrees of freedom in the system. The nature of this local moment could be revealed by looking at the respective magnetic and charge susceptibilities of the system, which are shown in Figs. 2(c)–2(f). It is seen that the local moment in the $U_{\rm eff} > 0$ regime is accompanied by formation of an orbital pseudospin magnetic moment in the system [see Fig. 2(c)]. On the other hand, in the $U_{\rm eff} < 0$ regime, we see that the established local moment is of charge type [see Fig. 2(f)].

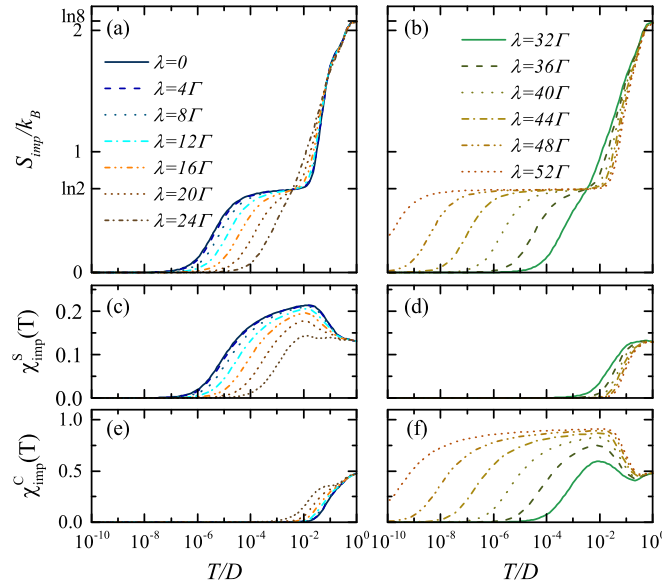

FIG. 2. Impurity contribution to the total entropy (top panels), magnetic susceptibility (middle panels) and charge susceptibility (bottom panels) of the system. The values of λ in the left and right panels correspond to the positive and negative $U_{\rm eff}$ regimes, respectively. Other parameters are $\varepsilon_1 = \varepsilon_2 = -U/2, U = 20\Gamma, \omega_0 = \lambda$, and $\Delta = 10\Gamma$.

Further decrease of the temperature results in fully screening this local moment, after which the system crosses over to its Kondo strong coupling fixed point with $S_{\rm imp} = 0$.

The particular temperature at which the local moment of the system quenches in Figs. 2(a) and 2(b) is usually called the Kondo temperature of the system. In Fig. 3(a), we show T_K values of the system calculated by the relation $S_{\rm imp}(T_K) = 0.5k_B \ln 2$ from NRG results. The dashed line shows the points on which the values of $U_{\rm eff}$ vanish. It is seen that the behavior of T_K values in the positive $U_{\rm eff}$ region differs from that in negative $U_{\rm eff}$ region. This is more obvious in Fig. 3(b), where we have plotted the details of Fig. 3(a) for a particular value of Δ. As we anticipated in Sec. III, in the positive $U_{\rm eff}$ region, increasing λ results in an increase of the T_K values, while, in the negative $U_{\rm eff}$ regime, the value of T_K is drastically decreased by increasing λ. In Fig. 3(b), we have also compared the NRG results with the results obtained using Eqs. (14) and (18), where we can see very good agreement between the two results. To complete our discussion about the Kondo temperature, in Fig. 3(c), we show the dependence of T_K on the values of V_z, where $V_z = (\varepsilon_1 - \varepsilon_2)/2$, and by assuming that the system is in the charge-Kondo regime. It is apparent that departures from $V_z = 0$ give rise to an enhancement of T_K, which is again in agreement with the results obtained using Eq. (18).

Next, we consider spectral and transport properties of the DQD. In Fig. 4, we show the spectral function of the DQD for different values of λ. Obviously, when the system is in the orbital-Kondo regime, $\lambda < 24\Gamma$, there is a central Kondo peak along with two sideband peaks which are placed at the energies corresponding to the single-particle excitation energies of the DQD. By increasing λ, the system slightly crosses over to the charge-Kondo regime, which is reflected in the central peak of the spectral function by first transforming it to a Lorentzian

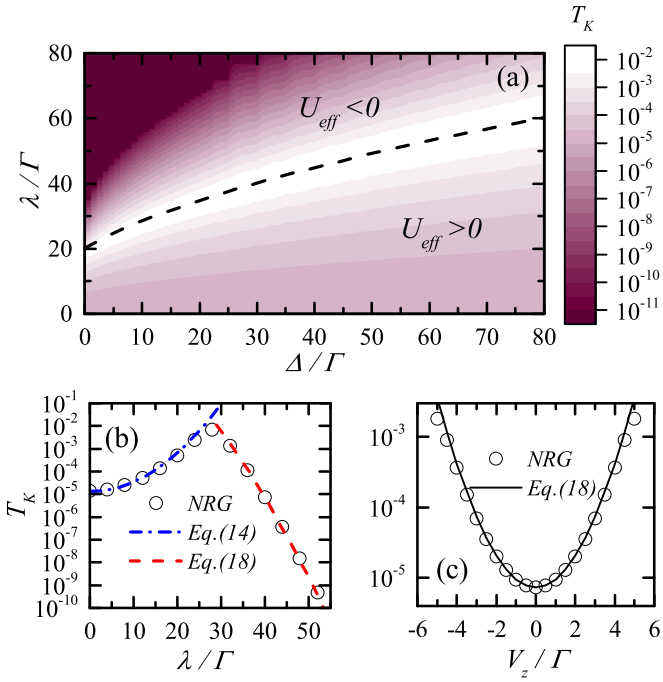

FIG. 3. (a) Kondo temperature of the system calculated from NRG results with respect to the λ and Δ. The dashed line shows the boundary between positive and negative U_{eff} regimes. (b) Comparison of Kondo temperature of the system for $\Delta = 10\Gamma$, calculated by NRG (circles), Eq. (14) (dash-dotted line), and Eq. (18) (dashed line). (c) Kondo temperature of the system as a function of V_z, calculated by NRG (circles) and Eq. (18) (dashed line), for $\Delta = 10\Gamma$, $\lambda = 40\Gamma$. The proportionality constants in Eqs. (14) and (18) are calculated by numerical fitting to be $\alpha = 0.034$ and $\beta = 0.016$. Other parameters are $\varepsilon_1 = \varepsilon_2 = -U/2$, $U = 20\Gamma$, $\omega_0 = \lambda$.

form around $\lambda \approx 28\Gamma$ and then to a sharp charge-Kondo peak for $\lambda > 32\Gamma$. Changing λ has also affected not only the energies but also the numbers of the sideband peaks. This behavior can be explained by considering the single-particle excitation energies of the isolated DQD-qubit, which could be calculated by using Eq. (7). In the orbital-Kondo regime, the ground state is the singly occupied states. Thus, there are four

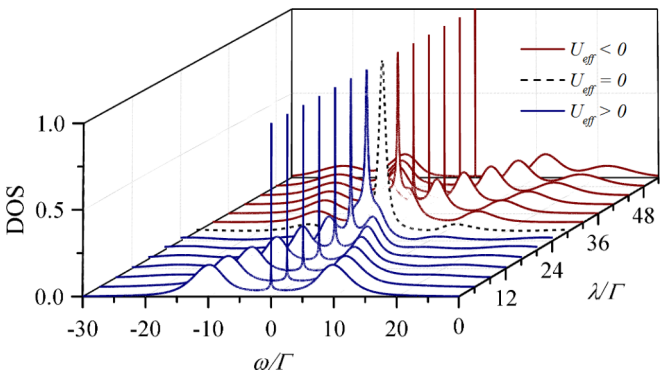

FIG. 4. The spectral function (DOS) of the DQD for λ values ranging from $\lambda = 0$ (orbital-Kondo regime) to $\lambda = 52\Gamma$ (charge-Kondo regime). The dashed line shows the DOS for the particular λ value corresponding to the vanishing U_{eff}. Other parameters are $\varepsilon_1 = \varepsilon_2 = -U/2$, $U = 20\Gamma$, $\omega_0 = \lambda$, $\Delta = 10\Gamma$.

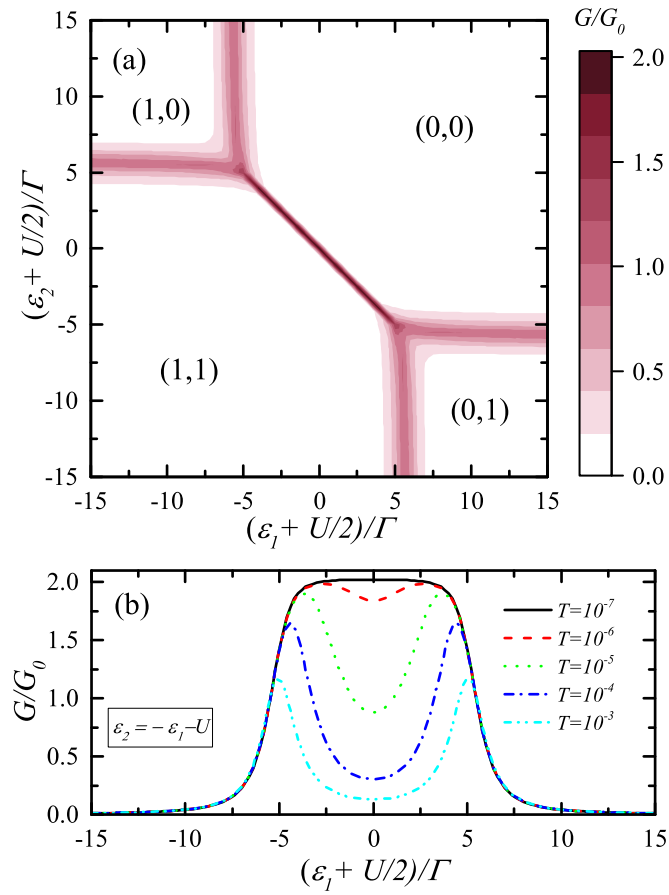

FIG. 5. (a) Total linear conductance of the DQD with respect to the ε_1 and ε_2 values. Charge configurations of the DQD are shown by (n_1,n_2) in the figure. (b) Temperature dependence of the total linear conductance of DQD along the diagonal line in (a). Other parameters are $U = 20\Gamma$, $\Delta = 10\Gamma$, $\omega_0 = \lambda$, and $\lambda = 40\Gamma$.

possible sideband peaks in this regime, with energies equal to $\pm|E_-^{1,0} - E_-^{0,0}|$ and $\pm|E_-^{1,0} - E_+^{0,0}|$, which are associated with the single-particle excitation in DQD without and with excitation of the qubit, respectively. However, as we can see in Fig. 4, in the orbital-Kondo regime, there are no sideband peaks with qubit excitation in the spectral function, which is mainly due to the weakness of the DQD-qubit coupling. For larger λ values, and specifically in the charge-Kondo regime, the sideband peaks with qubit excitation are much more visible. We note that in the charge-Kondo regime, the ground state is composed of the empty and doubly occupied states, and therefore the sideband peaks energies are obtained from $\pm|E_-^{0,0} - E_-^{1,0}|$ and $\pm|E_-^{0,0} - E_+^{1,0}|$.

In Fig. 5(a), we show the total conductance of the DQD (G) in the ε_1-ε_2 plane. The parameters are chosen such that the system is in the $U_{\text{eff}} < 0$ regime. We see that the profile of the total conductance is rotated with respect to the usual charge stability diagrams expected for an interacting parallel DQD [39]. In particular, the presence of a long degeneracy between the two charge configurations (0,0) and (1,1) is a clue of an attractive interaction in the DQD. We can also infer the strength of this attractive interaction as the length of this degeneracy line segment between the two (0,0) and (1,1) regions. We show the

temperature dependence of G along this segment in Fig. 5(b), in which we can see that the conductance on this segment reaches the unitary value $G = 2G_0 = 2e^2/h$ for low enough temperatures, while for higher temperatures it is suppressed except at the end points of the degeneracy segment. Hence, from these observations, we can deduce that the nature of this unitary conductance is of charge-Kondo type. It should be emphasized that a similar conductance enhancement was reported in Ref. [34].

V. CONCLUSIONS

In conclusion, we considered a double quantum dot which is capacitively coupled to a charge qubit. It is shown that this capacitive coupling renormalizes the interdot repulsive interaction in the double quantum dot and in some situations makes it an attractive interaction between the electrons in the double quantum dot. We found that appropriate coupling of the double quantum dot with the electrodes could give rise to two different types of the Kondo effect depending on the sign of the interdot interaction in the double quantum dot. Namely, in the positive interaction regime, the system shows an isotropic orbital-Kondo effect while, in the negative interaction regime, an anisotropic charge-Kondo effect is expected to be shown in the system. By deriving the low-energy effective Hamiltonian of the system, we obtained the corresponding Kondo exchange coupling constants as well as the characteristic Kondo temperature of the system corresponding to these two different regimes. Moreover, we employed the numerical renormalization group method to confirm our analytical results and to extract some thermodynamic and electronic transport properties of the system.

ACKNOWLEDGMENTS

We would like to thank Farshad Ebrahimi for bringing the importance of the model system to our attention. We are also grateful to Pablo S. Cornaglia for useful comments and critical reading of a previous version of the manuscript and to Rok Žitko for helpful comments.

APPENDIX: DERIVATION OF EFFECTIVE HAMILTONIAN

The low-energy effective Hamiltonian of the system can be calculated using the method of degenerate perturbation theory. We will calculate the second-order corrections to the unperturbed subsystem $\hat{\mathcal{H}}_0 = \hat{\mathcal{H}}_S + \hat{\mathcal{H}}_L$ due to the perturbation coming from electron transitions between DQD and electrodes, which is described by $\hat{\mathcal{H}}_T$. First, for future reference, we define eight projection operators to the subspace of the eigenstates $|\psi_\pm^{n_1,n_2}\rangle$ by

$$\hat{P}_\pm^{0,0} = (1-\hat{n}_1)(1-\hat{n}_2)|0,\pm\rangle\langle 0,\pm|, \tag{A1a}$$

$$\hat{P}_\pm^{1,0} = \hat{n}_1(1-\hat{n}_2)|1,\pm\rangle\langle 1,\pm|, \tag{A1b}$$

$$\hat{P}_\pm^{0,1} = (1-\hat{n}_1)\hat{n}_2|1,\pm\rangle\langle 1,\pm|, \tag{A1c}$$

$$\hat{P}_\pm^{1,1} = \hat{n}_1\hat{n}_2|2,\pm\rangle\langle 2,\pm|. \tag{A1d}$$

Now, the correction to the $\hat{\mathcal{H}}_0$ to the lowest order in $\hat{\mathcal{H}}_T$ can be calculated by [30,36]

$$\hat{\mathcal{H}}_{\text{eff}} = \sum_{\substack{n_1,n_2=0,1\\ \nu=\pm}} \frac{\hat{P}_0\hat{\mathcal{H}}_T\hat{P}_\nu^{n_1,n_2}\hat{\mathcal{H}}_T\hat{P}_0}{E_0 - E_\nu^{n_1,n_2}}, \tag{A2}$$

where $\hat{P}_0$ denotes the projection to the specific ground-state of the unperturbed Hamiltonian $\hat{\mathcal{H}}_0$ with energy E_0. Because we are interested in deriving the Kondo Hamiltonian, we restrict our calculations to the degenerate ground states in the following discussions.

1. Positive U_{eff} regime

In this regime, the ground state becomes degenerate when $E_-^{1,0} = E_-^{0,1}$, $E_-^{1,0} < E_-^{0,0}$, and $E_-^{1,0} < E_-^{1,1}$. Due to the large number of available parameters in the system, various parameter configurations can fulfill these conditions. By fixing $\lambda = \omega_0$, which makes the qubit particle-hole symmetric, we find that the necessary conditions for degeneracy in the ground state become $\varepsilon_1 = \varepsilon_2 = V_g$ and $|\varepsilon_1 + \frac{U}{2}| < \frac{1}{2}(U + \Omega_1 - \Omega_0)$, where we have allowed for a gate voltage V_g to consider the general case. By denoting the ground-state projector as $\hat{P}_0 = \hat{P}_-^{1,0} + \hat{P}_-^{0,1}$, we can evaluate the effective Hamiltonian in this case by

$$\hat{\mathcal{H}}_{\text{eff}} = \sum_{\substack{n_1,n_2=0,1\\ \nu=\pm}} \frac{\langle 1,-|(\hat{P}_-^{1,0}+\hat{P}_-^{0,1})\hat{\mathcal{H}}_T\hat{P}_\nu^{n_1,n_2}\hat{\mathcal{H}}_T(\hat{P}_-^{1,0}+\hat{P}_-^{0,1})|1,-\rangle}{E_-^{1,0} - E_\nu^{n_1,n_2}}. \tag{A3}$$

Note that we have traced out the qubit's degrees of freedom in order to obtain a pure electronic effective Hamiltonian. Explicit calculation of different terms in the above relation leads to

$$\sum_{\nu=\pm} \frac{\langle 1,-|(\hat{P}_-^{1,0}+\hat{P}_-^{0,1})\hat{\mathcal{H}}_T\hat{P}_\nu^{0,0}\hat{\mathcal{H}}_T(\hat{P}_-^{1,0}+\hat{P}_-^{0,1})|1,-\rangle}{E_-^{1,0} - E_\nu^{0,0}} = \frac{4t^2(-\Delta+V_g)}{4V_g(\Delta-V_g)+\lambda^2}$$
$$\times \sum_{i=1,2}[-\delta_{q,p}(\hat{n}_i - \hat{n}_1\hat{n}_2) + \hat{\tilde{c}}_{q,i}^\dagger\hat{\tilde{c}}_{p,i}\hat{n}_i + \hat{\tilde{c}}_{q,i}^\dagger\hat{\tilde{c}}_{p,\bar{i}}\hat{d}_{\bar{i}}^\dagger\hat{d}_i - \hat{\tilde{c}}_{q,i}^\dagger\hat{\tilde{c}}_{p,i}\hat{n}_1\hat{n}_2], \tag{A4a}$$

$$\sum_{\nu=\pm}\frac{\langle 1,-|(\hat{P}_-^{1,0}+\hat{P}_-^{0,1})\hat{\mathcal{H}}_T\hat{P}_\nu^{1,1}\hat{\mathcal{H}}_T(\hat{P}_-^{1,0}+\hat{P}_-^{0,1})|1,-\rangle}{E_-^{1,0}-E_\nu^{1,1}}=\frac{4t^2(\Delta+V_g+U)}{4(V_g+U)(\Delta+V_g+U)-\lambda^2}$$
$$\times\sum_{i=1,2}[-\hat{\tilde{c}}_{q,i}^\dagger\hat{\tilde{c}}_{p,i}\hat{n}_{\bar{i}}+\hat{\tilde{c}}_{q,i}^\dagger\hat{\tilde{c}}_{p,\bar{i}}\hat{d}_{\bar{i}}^\dagger\hat{d}_i+\hat{\tilde{c}}_{q,i}^\dagger\hat{\tilde{c}}_{p,i}\hat{n}_1\hat{n}_2]. \tag{A4b}$$

Summing the above two contributions to the effective Hamiltonian and using the identities $\hat{n}_1\hat{n}_2=1-\hat{n}_d$ and $\hat{n}_d=1$ which are valid only in the ground-state subspace of the positive $U_{\rm eff}$ regime, we can reach to the following expression for $\hat{\mathcal{H}}_{\rm eff}$:

$$\hat{\mathcal{H}}_{\rm eff}=J\,\vec{S}_d\cdot\vec{S}_c+K\sum_{\substack{i,j=1,2\\q,p}}\hat{\tilde{c}}_{q,i}^\dagger\hat{\tilde{c}}_{p,i}/2, \tag{A5}$$

where J and K are given by

$$J=\frac{t^2}{(V_g+U)-\frac{(\lambda/2)^2}{\Delta+V_g+U}}-\frac{t^2}{V_g-\frac{(\lambda/2)^2}{V_g-\Delta}}, \tag{A6a}$$
$$K=\frac{t^2}{(V_g+U)-\frac{(\lambda/2)^2}{\Delta+V_g+U}}+\frac{t^2}{V_g-\frac{(\lambda/2)^2}{V_g-\Delta}}. \tag{A6b}$$

Moreover, $\vec{S}_d=\frac{1}{2}\sum_{i,j=1,2}\hat{d}_i^\dagger\vec{\sigma}_{ij}\hat{d}_j$ is the corresponding pseudospin vector of the DQD, which is represented by

$$S_d^x=\tfrac{1}{2}(\hat{d}_2^\dagger\hat{d}_1+\hat{d}_2^\dagger\hat{d}_1), \tag{A7a}$$
$$S_d^y=\tfrac{i}{2}(\hat{d}_2^\dagger\hat{d}_1-\hat{d}_2^\dagger\hat{d}_1), \tag{A7b}$$
$$S_d^z=\tfrac{1}{2}(\hat{n}_1-\hat{n}_2), \tag{A7c}$$

and, analogously, $\vec{S}_c=\frac{1}{2}\sum_{i,j=1,2}\sum_{p,q}\hat{\tilde{c}}_{q,i}^\dagger\vec{\sigma}_{ij}\hat{\tilde{c}}_{p,j}$ is the pseudospin vector for the electrodes.

2. Negative $U_{\rm eff}$ regime

In this regime, a calculation similar to that of the positive $U_{\rm eff}$ regime but for the the ground state composed of the two states $|\psi_-^{0,0}\rangle$ and $|\psi_-^{1,1}\rangle$ leads to the conditions $\lambda=\omega_0$, $\varepsilon_1+\varepsilon_2+U=0$ and $|V_z|<\frac{1}{2}(-U-\Omega_1+\Omega_0)$, where $V_z=\varepsilon_1+U/2=-(\varepsilon_2+U/2)$. Then, the ground-state projector is $\hat{P}_0=\hat{P}_-^{0,0}+\hat{P}_-^{1,1}$, and the effective Hamiltonian can be calculated by

$$\hat{\mathcal{H}}_{\rm eff}=\sum_{\substack{n_1,n_2=0,1\\\nu=\pm}}\frac{(\langle 0,-|\hat{P}_-^{0,0}+\langle 2,-|\hat{P}_-^{1,1})\hat{\mathcal{H}}_T\hat{P}_\nu^{n_1,n_2}\hat{\mathcal{H}}_T(\hat{P}_-^{0,0}|0,-\rangle+\hat{P}_-^{1,1}|2,-\rangle)}{E_-^{0,0}-E_\nu^{n_1,n_2}}. \tag{A8}$$

By calculating the summations in the above relation, after some algebra, we get

$$\sum_{\nu=\pm}\frac{\langle 0,-|\hat{P}_-^{0,0}\hat{\mathcal{H}}_T\hat{P}_\nu^{1,0}\hat{\mathcal{H}}_T\hat{P}_-^{0,0}|0,-\rangle}{E_-^{0,0}-E_\nu^{1,0}}+\frac{\langle 2,-|\hat{P}_-^{1,1}\hat{\mathcal{H}}_T\hat{P}_\nu^{1,0}\hat{\mathcal{H}}_T\hat{P}_-^{1,1}|2,-\rangle}{E_-^{0,0}-E_\nu^{1,0}}$$
$$=\frac{2t^2}{\Delta^2-(-U+2V_z+\Omega_0)^2}\left(\lambda-U+2V_z+\frac{\Delta^2(\lambda+2\Omega_0)}{\left(\Delta^2+\lambda^2+\lambda\Omega_0\right)}\right)$$
$$\times[\hat{\tilde{c}}_{q,1}^\dagger\hat{\tilde{c}}_{p,1}-\hat{\tilde{c}}_{q,1}^\dagger\hat{\tilde{c}}_{p,1}\hat{n}_d+\delta_{q,p}\hat{n}_1\hat{n}_2+(\hat{\tilde{c}}_{q,1}^\dagger\hat{\tilde{c}}_{p,1}-\hat{\tilde{c}}_{q,2}^\dagger\hat{\tilde{c}}_{p,2})\hat{n}_1\hat{n}_2], \tag{A9a}$$

$$\sum_{\nu=\pm}\frac{\langle 0,-|\hat{P}_-^{0,0}\hat{\mathcal{H}}_T\hat{P}_\nu^{0,1}\hat{\mathcal{H}}_T\hat{P}_-^{0,0}|0,-\rangle}{E_-^{0,0}-E_\nu^{0,1}}+\frac{\langle 2,-|\hat{P}_-^{1,1}\hat{\mathcal{H}}_T\hat{P}_\nu^{0,1}\hat{\mathcal{H}}_T\hat{P}_-^{1,1}|2,-\rangle}{E_-^{0,0}-E_\nu^{0,1}}$$
$$=\frac{2t^2}{\Delta^2-(U+2V_z-\Omega_0)^2}\left(\lambda-U-2V_z+\frac{\Delta^2(\lambda+2\Omega_0)}{\left(\Delta^2+\lambda^2+\lambda\Omega_0\right)}\right)$$
$$\times[\hat{\tilde{c}}_{q,2}^\dagger\hat{\tilde{c}}_{p,2}-\hat{\tilde{c}}_{q,2}^\dagger\hat{\tilde{c}}_{p,2}\hat{n}_d+\delta_{q,p}\hat{n}_1\hat{n}_2+(\hat{\tilde{c}}_{q,2}^\dagger\hat{\tilde{c}}_{p,2}-\hat{\tilde{c}}_{q,1}^\dagger\hat{\tilde{c}}_{p,1})\hat{n}_1\hat{n}_2], \tag{A9b}$$

$$\sum_{\nu=\pm}\frac{\langle 0,-|\hat{P}_{-}^{0,0}\hat{\mathcal{H}}_T\hat{P}_{\nu}^{0,1}\hat{\mathcal{H}}_T\hat{P}_{-}^{1,1}|2,-\rangle}{E_{-}^{0,0}-E_{\nu}^{0,1}}+\frac{\langle 2,-|\hat{P}_{-}^{1,1}\hat{\mathcal{H}}_T\hat{P}_{\nu}^{0,1}\hat{\mathcal{H}}_T\hat{P}_{-}^{0,0}|0,-\rangle}{E_{-}^{0,0}-E_{\nu}^{0,1}}$$

$$=\frac{2\Delta t^2/\Omega_0}{2V_z-U+\frac{\lambda^2}{2V_z-U+2\Omega_0}}\sum_{i=1,2}[\hat{\tilde{c}}_{q,i}^{\dagger}\hat{\tilde{c}}_{p,\bar{i}}^{\dagger}\hat{d}_{\bar{i}}\hat{d}_i+\text{H.c.}], \tag{A9c}$$

$$\sum_{\nu=\pm}\frac{\langle 0,-|\hat{P}_{-}^{0,0}\hat{\mathcal{H}}_T\hat{P}_{\nu}^{1,0}\hat{\mathcal{H}}_T\hat{P}_{-}^{1,1}|2,-\rangle}{E_{-}^{0,0}-E_{\nu}^{1,0}}+\frac{\langle 2,-|\hat{P}_{-}^{1,1}\hat{\mathcal{H}}_T\hat{P}_{\nu}^{1,0}\hat{\mathcal{H}}_T\hat{P}_{-}^{0,0}|0,-\rangle}{E_{-}^{0,0}-E_{\nu}^{1,0}}$$

$$=\frac{-2\Delta t^2/\Omega_0}{2V_z+U+\frac{\lambda^2}{2V_z+U-2\Omega_0}}\sum_{i=1,2}[\hat{\tilde{c}}_{q,i}^{\dagger}\hat{\tilde{c}}_{p,\bar{i}}^{\dagger}\hat{d}_{\bar{i}}\hat{d}_i+\text{H.c.}]. \tag{A9d}$$

Now, by defining the isospin operators $\overrightarrow{I}_d$ of the DQD as

$$I_d^x=\tfrac{1}{2}(\hat{d}_2^{\dagger}\hat{d}_1^{\dagger}+\hat{d}_1\hat{d}_2), \tag{A10a}$$

$$I_d^y=\tfrac{i}{2}(\hat{d}_2^{\dagger}\hat{d}_1^{\dagger}-\hat{d}_1\hat{d}_2), \tag{A10b}$$

$$I_d^z=\tfrac{1}{2}(\hat{n}_d-1), \tag{A10c}$$

with a similar definition for the $\overrightarrow{I}_c$ as the iso-spin operators of the electrodes and using the identities $2\hat{n}_1\hat{n}_2=\hat{n}_d$ and $\hat{n}_1=\hat{n}_2$ which are valid in the ground state of the negative U_{eff} regime, we can obtain the effective Hamiltonian in Eq. (16).

[1] A. C. Hewson, *The Kondo Problem to Heavy Fermions*, Vol. 2, (Cambridge University Press, Cambridge, 1997).
[2] T. W. Odom, J.-L. Huang, C. L. Cheung, and C. M. Lieber, Science **290**, 1549 (2000).
[3] M. R. Buitelaar, T. Nussbaumer, and C. Schönenberger, Phys. Rev. Lett. **89**, 256801 (2002).
[4] L. H. Yu and D. Natelson, Nano Lett. **4**, 79 (2004).
[5] R. Potok, I. Rau, H. Shtrikman, Y. Oreg, and D. Goldhaber-Gordon, Nature (London) **446**, 167 (2007).
[6] Y.-S. Fu, S.-H. Ji, X. Chen, X.-C. Ma, R. Wu, C.-C. Wang, W.-H. Duan, X.-H. Qiu, B. Sun, P. Zhang *et al.*, Phys. Rev. Lett. **99**, 256601 (2007).
[7] M. R. Calvo, J. Fernandez-Rossier, J. J. Palacios, D. Jacob, D. Natelson, and C. Untiedt, Nature (London) **458**, 1150 (2009).
[8] J. Pillet, C. Quay, P. Morfin, C. Bena, A. L. Yeyati, and P. Joyez, Nat. Phys. **6**, 965 (2010).
[9] E. J. H. Lee, X. Jiang, M. Houzet, R. Aguado, C. M. Lieber, and S. De Franceschi, Nat. Nanotechnol. **9**, 79 (2014).
[10] Z. Iftikhar, S. Jezouin, A. Anthore, U. Gennser, F. Parmentier, A. Cavanna, and F. Pierre, Nature (London) **526**, 233 (2015).
[11] T. Inoshita, Science **281**, 526 (1998).
[12] S. M. Cronenwett, T. H. Oosterkamp, and L. P. Kouwenhoven, Science **281**, 540 (1998).
[13] M. Pustilnik and L. Glazman, J. Phys.: Condens. Matter **16**, R513(R) (2004).
[14] P. Jarillo-Herrero, J. Kong, H. S. Van Der Zant, C. Dekker, L. P. Kouwenhoven, and S. De Franceschi, Nature (London) **434**, 484 (2005).
[15] S. Amasha, A. J. Keller, I. G. Rau, A. Carmi, J. A. Katine, H. Shtrikman, Y. Oreg, and D. Goldhaber-Gordon, Phys. Rev. Lett. **110**, 046604 (2013).
[16] Z.-q. Bao, A.-M. Guo, and Q.-f. Sun, J. Phys.: Condens. Matter **26**, 435301 (2014).
[17] A. Taraphder and P. Coleman, Phys. Rev. Lett. **66**, 2814 (1991).
[18] Y. Matsushita, H. Bluhm, T. H. Geballe, and I. R. Fisher, Phys. Rev. Lett. **94**, 157002 (2005).
[19] M. Dzero and J. Schmalian, Phys. Rev. Lett. **94**, 157003 (2005).
[20] M. Matusiak, E. M. Tunnicliffe, J. R. Cooper, Y. Matsushita, and I. R. Fisher, Phys. Rev. B **80**, 220403 (2009).
[21] T. A. Costi and V. Zlatić, Phys. Rev. Lett. **108**, 036402 (2012).
[22] G. Cheng, M. Tomczyk, S. Lu, J. P. Veazey, M. Huang, P. Irvin, S. Ryu, H. Lee, C.-B. Eom, C. S. Hellberg *et al.*, Nature (London) **521**, 196 (2015).
[23] G. E. Prawiroatmodjo, M. Leijnse, F. Trier, Y. Chen, D. V. Christensen, M. Soosten, N. Pryds, and T. S. Jespersen, Nat Commun. **8**, 395 (2017).
[24] T.-F. Fang, A.-M. Guo, H.-T. Lu, H.-G. Luo, and Q.-F. Sun, Phys. Rev. B **96**, 085131 (2017).
[25] L. Borda, G. Zaránd, W. Hofstetter, B. I. Halperin, and J. von Delft, Phys. Rev. Lett. **90**, 026602 (2003).
[26] A. S. Alexandrov, A. M. Bratkovsky, and R. S. Williams, Phys. Rev. B **67**, 075301 (2003).
[27] P. S. Cornaglia, H. Ness, and D. R. Grempel, Phys. Rev. Lett. **93**, 147201 (2004).
[28] M. R. Galpin, D. E. Logan, and H. R. Krishnamurthy, Phys. Rev. Lett. **94**, 186406 (2005).
[29] D. E. Liu, S. Chandrasekharan, and H. U. Baranger, Phys. Rev. Lett. **105**, 256801 (2010).
[30] I. Garate, Phys. Rev. B **84**, 085121 (2011).
[31] S. Andergassen, T. A. Costi, and V. Zlatić, Phys. Rev. B **84**, 241107 (2011).

[32] G. Yoo, J. Park, S.-S. B. Lee, and H.-S. Sim, Phys. Rev. Lett. **113**, 236601 (2014).
[33] G. Széchenyi, A. Pályi, and M. Droth, Phys. Rev. B **96**, 245302 (2017).
[34] A. Hamo, A. Benyamini, I. Shapir, I. Khivrich, J. Waissman, K. Kaasbjerg, Y. Oreg, F. von Oppen, and S. Ilani, Nature (London) **535**, 395 (2016).
[35] W. Little, Phys. Rev. **134**, A1416 (1964).
[36] J. S. Lim, R. López, G. Platero, and P. Simon, Phys. Rev. B **81**, 165107 (2010).
[37] R. Bulla, T. A. Costi, and T. Pruschke, Rev. Mod. Phys. **80**, 395 (2008).
[38] R. Žitko, http://nrgljubljana.ijs.si/.
[39] W. G. Van der Wiel, S. De Franceschi, J. M. Elzerman, T. Fujisawa, S. Tarucha, and L. P. Kouwenhoven, Rev. Mod. Phys. **75**, 1 (2002).